

ChemComm

Accepted Manuscript



This is an *Accepted Manuscript*, which has been through the Royal Society of Chemistry peer review process and has been accepted for publication.

Accepted Manuscripts are published online shortly after acceptance, before technical editing, formatting and proof reading. Using this free service, authors can make their results available to the community, in citable form, before we publish the edited article. We will replace this *Accepted Manuscript* with the edited and formatted *Advance Article* as soon as it is available.

You can find more information about *Accepted Manuscripts* in the [Information for Authors](#).

Please note that technical editing may introduce minor changes to the text and/or graphics, which may alter content. The journal's standard [Terms & Conditions](#) and the [Ethical guidelines](#) still apply. In no event shall the Royal Society of Chemistry be held responsible for any errors or omissions in this *Accepted Manuscript* or any consequences arising from the use of any information it contains.

COMMUNICATION

Reversible Crystal Deformation of a Single-Crystal Host of Copper(II)1-Naphthoate—Pyrazine through Crystal Phase Transition Induced by Methanol Vapor Sorption

Cite this: DOI: 10.1039/x0xx00000x

Received 00th January 2012,

Accepted 00th January 2012

DOI: 10.1039/x0xx00000x

www.rsc.org/

Yuichi Takasaki^a and Satoshi Takamizawa^{*a}

A novel microporous single crystal of [Cu(II)₂(1-NA)₄(pyz)]_n (1-NA: 1-naphthoate, pyz: pyrazine) exhibited bending and straightening action on a macroscopic scale during the first-order crystal phase transition induced by methanol vapor sorption.

Microporous metal complexes are regarded as functional materials for gas storage, gas separation, and catalysts¹ due to their designable pore structures compared with conventional porous solids, such as zeolites or activated carbons.² Recently, there have been an increasing number of reports of single-crystal-to-single-crystal transition induced by gas adsorption in microporous metal complexes, which correlate with discontinuous changes of the properties of a solid (shape, color, electric conductivity, and magnetism).³ Crystal deformation of the microporous materials induced by crystal phase transition can be utilized for crystalline devices such as sensors or actuators. A step-wise adsorption profile is regarded as a typical indication of crystal phase change and is known as a so-called “gate-opening” type isotherm.⁴ Our group proposed a “mass-induced phase transition” mechanism for such behavior, which suggested the coexisting state of two different host crystal phases under the transition state.⁵ Although crystal deformation or crystal structural changes during gas adsorption and/or desorption were observed,⁶ the precise understanding of macroscopic crystal deformation mediated by crystal phase transition during gas sorption is not clear. Combined *in situ* observation of the crystal deformation under an optical microscope and a single-crystal X-ray diffractometer can clarify the correlation between gas sorption and crystal transformation. Our group previously reported that a flexible metal complex of [Cu(II)₂(bza)₄(pyz)]_n (bza: benzoate, pyz: pyrazine) and its derivatives generated stable guest inclusion crystals for various inorganic gases and organic vapors while preserving single solid morphologies, and have clarified that the gases diffuse inside the channel space by a gas permeation method performed on the single-crystal membranes.⁷

In this study, we synthesized a novel molecular crystal of [Cu(II)₂(1-NA)₄(pyz)]_n (1-NA: 1-naphthoate) (**1**) and succeeded in *in situ* observation of the crystal deformation of **1** through gaseous guest ad- and desorption under a microscope and single-crystal X-ray

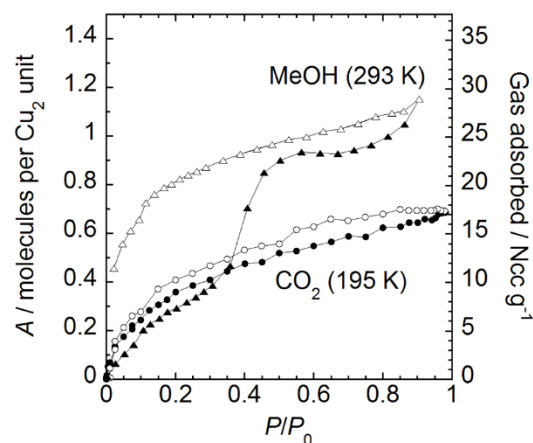


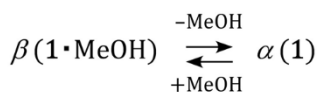
Fig. 1 Adsorption (filled plots) and desorption (open plots) isotherm of methanol vapor at 293 K (triangle) and CO₂ at 195 K (circle).

diffraction measurement for the guest inclusion crystal.

Microcrystals of **1**⁸ adsorbed CO₂ gas with a slight hysteresis in the isotherm curve at 195 K. (Fig. 1) The adsorption amount of CO₂ gas finally reached 17.2 cc g⁻¹ or 0.71 molecule per Cu₂ unit at a relative pressure (P/P_0) of 0.99. In contrast, **1** adsorbed methanol vapor with a step-wise isotherm curve at 293 K, which is an indication of crystal phase transition. The adsorption amount of methanol molecules started to increase abruptly from 11.7 cc g⁻¹ or 0.48 molecule per Cu₂ unit at $P/P_0 = 0.35$ and finally reached 29.0 cc g⁻¹ or 1.2 molecules per Cu₂ unit at $P/P_0 = 0.9$. The critical pressure for the abrupt increase in the adsorption process is quite similar to that of acetonitrile sorption in [Cu(II)₂(bza)₄(pyz)]_n ($P/P_0 = 0.45$ at 293 K).⁹ The maximum adsorbed number of methanol molecules in **1** agreed well with the numbers based on the X-ray data described later. During the abrupt increase in the adsorption amount, a two-phase coexisting state in the style of first-order transition is expected to be observed in the single crystal. In the desorption process, an abrupt decrease indicating the reverse transition from the sorbed

phase to the vacant phase was observed at less than 18.2 cc g^{-1} at $P/P_0 = 0.11$, causing a wide pressure width in the hysteresis loop. This indicated difficulty in the guest diffusion during the desorption process. Methanol vapor is an adequate guest for observing crystal transformation during the phase transition of **1** because of the moderate speed of its sorption at room temperature. It shows promise for clarifying the correlation between gas sorption and crystal deformation.

As expected from the observed step-wise adsorption isotherm of methanol vapor, the single-crystal-to-single-crystal phase transition of **1** was confirmed by single-crystal X-ray diffraction measurements for the synthesized crystal including methanol as a crystal solvent and the dried crystal after vacuum drying. The crystal phases are denoted as β phase (**1**•MeOH) and α phase (**1**). (X-ray data suggested the composition of **1**•0.93(MeOH) for the β crystal.¹⁰)



Scheme 1

The crystal structure of the β phase (triclinic, $P-1$) at 90 K was a methanol-containing structure with a unit-cell volume of 2066.2 \AA^3 , which was formed by 1D chains in which the paddle-wheel units (binuclear Cu_2 center with four 1-NA) were bridged by pyz. (Figure 2a) The 1D chains have a uniform zigzag shape with a bending angle of 5.33° and are associated by π - π interactions between neighboring naphthalene moieties (colored red, blue, green, and pink in Fig. 2a) to form isolated voids surrounded by naphthalene planes. The total number of methanol molecules included in the two voids in a unit cell was estimated as 1 molecule per Cu_2 unit, which agreed with the maximum value of 1.2 molecules per Cu_2 unit observed in methanol vapor adsorption measurements at 293 K.¹¹

The crystal structure of the α phase (triclinic, $P-1$) at 90 K observed after vacuum drying was a vacant structure with a unit-cell volume of 1982.5 \AA^3 and was inherently unchanged from the structure of the β phase but the conformation of the 1D chain was transformed through shrinking of the void spaces by losing the included methanol molecules. (Fig. 2b) Considering structural changes from the β phase to the α phase, the bending angle of the zigzag 1D chain of the β phase (5.33°) increased to that of the α phase (10.08°) with adjustment of the orientation of the naphthalene planes to preserve π - π interactions, which decreased

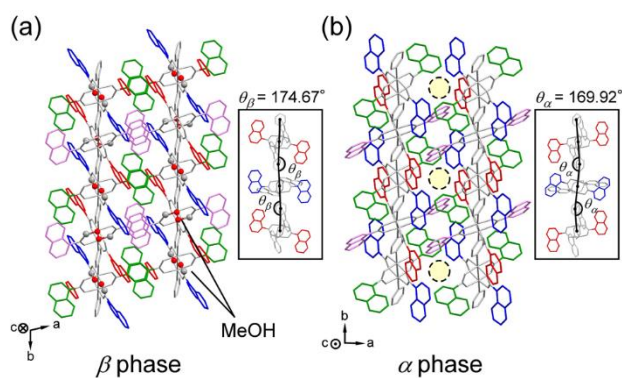


Fig. 2 Packing structures of (a) β phase (**1**•MeOH) and (b) α phase (**1**) viewed along each c axis. Inset figures represent the bending angle of zigzag 1D chains.

the void spaces from 217.2 \AA^3 (β) to 133.9 \AA^3 (α) in each unit cell but opened the neck diameter (ϕ) from less than 0.2 \AA (β) to 1.4 \AA (α). Therefore, the nearly isolated voids in the β phase shrank and transformed into the 1D channel connected by the neck moieties (ϕ : 1.4 \AA) in the α phase.

In the *in situ* observation of desorbing the included methanol solution from an as-synthesized single crystal of **1** under a polarizing microscope in bright field illumination with vacuum drying at 100°C , the α and β phases coexisted as a stripe pattern with a light-dark boundary and the crystal shape became a bent shape with the formation of planar α/β interfaces. (Movie S1) At the beginning of crystal deformation, the top of the α crystal domains appeared from $(0-11)_\beta$ or $(01-1)_\beta$, after which they became narrow, straight domains. After drying for 3 hours, the planar α/β interfaces transferred with a velocity of $4 \mu\text{m}$ per hour for one edge of the moving interfaces, and the areas of the α crystal domains widened. (Fig. 3a (i-ii)) Although a narrow α crystal domain hardly contributed any obvious change in crystal shape, the crystal macroscopically deformed into a bent shape under the α - β coexisting state after the α crystal domains condensed by continuous vacuum drying for 1 day. (Fig. 3a (iii)) The bending angle of the crystal was 12° at each position of the α - β boundary. (Enlarged images in the right of Fig. 3a) In the reverse process, by introducing methanol vapor into the bent crystal at 25°C for 6 hours, the α crystal domains started to contract at 50 Torr ($P/P_0 = 0.39$), and the crystal shape recovered to its straight form, (Fig. 3a (iii-iv)) which is reasonable based on the critical pressure ($P/P_0 = 0.35$) of the methanol vapor adsorption isotherm. (Fig. 1) After the saturated pressure of methanol vapor (127 Torr) at 25°C was reached, the crystal shape nearly recovered to its straight shape.¹² (Fig. 3a (v)) The

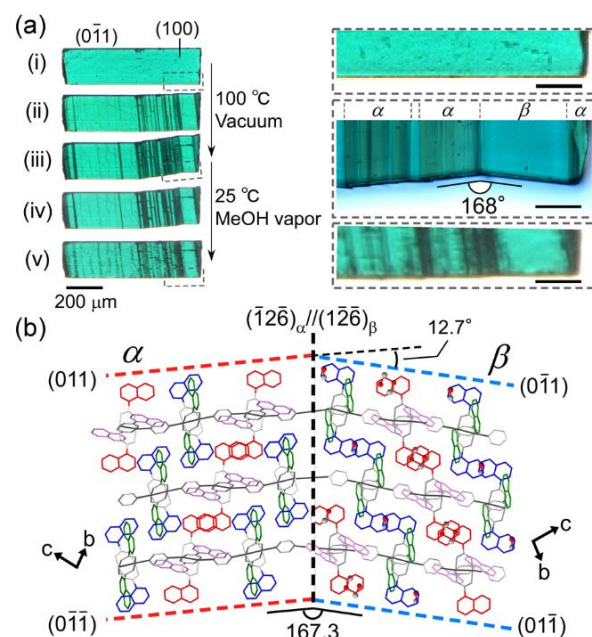


Fig. 3 (a) Bending and straightening process of **1** observed under a polarized microscope. The right figures are enlarged images of the marked portions of the left images of i, iii, and v (scale bars in enlarged figure are $30 \mu\text{m}$). (b) Connection of packing structures of α and β phases on the interface.

existence of definite planar interfaces under the α - β coexisting state without crystal cleavage indicated a regular connection of the α and β phases.

Crystal face indexing in the α - β coexisting state explains the mechanism of crystal bending. The planar α/β interface was determined as $(-12-6)_\alpha // (1-2-6)_\beta$, which runs across 1D chains along a plane consisting of copper atoms and nitrogen atoms of neighboring 1D chains. (Fig. 3b) The 1D chains were equally connected at the interface with an angle of 12.7° estimated from the projected directions of $[100]_\alpha$ and $[100]_\beta$ in Fig. 3b, which agrees with the macroscopic bending angle of 12° measured under a microscope. This suggested that the interface correspondence determines the macroscopic bending shape of the single crystal while sorbing gas. On the observed α/β interface, the interchain distances of the α phase are shorter than are those of the β phase by 0.19 \AA at 90 K as the averaged differential length, and the difference of interchain distance provides the smallest boundary strain of 3.6% on the interface by a ratio of $101.8 \text{ \AA}^2 (\alpha) / 105.6 \text{ \AA}^2 (\beta)$.¹³ Therefore, the interfaces under the α - β coexisting state appeared as the planar form so as to minimize the boundary strain on the interface.

The difficulty in desorbing methanol molecules for initiating β -to- α transition can be explained by the difference of guest diffusivity in the α and β crystals in considering differences in void structures. (Fig. 4) In the methanol adsorption process, the narrow voids with open necks in the α phase allow the moderate diffusivity of guest molecules, which supplies the guest molecules for generating β phase possessing-expanded voids in the shuttering necks. The change in pore morphologies from the α to β phase is similar to the closing of a drawstring bag to hold objects. Thus, in the methanol desorption process, an excess lowering of pressure is required to surpass the activation barrier to regain guest diffusivity by opening the closed necks accompanying crystal transition, which results in the large hysteresis loop. Additionally, the striped pattern of domain topology in the α - β coexisting state where the channels in an α crystal are blocked by the two neighboring β crystals tilts the slope of the desorption curve during β -to- α transition.

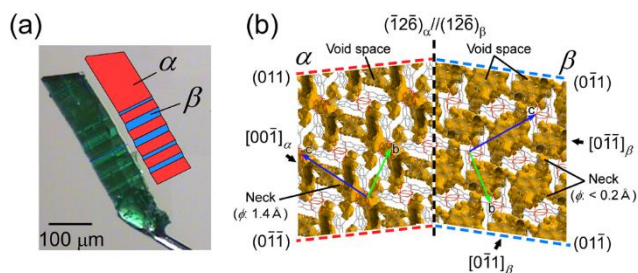


Fig. 4 (a) Single crystal of **1** under α - β coexisting state used for crystal face indexing. (b) Connections of pore structures on the interface. (Yellow regions are void spaces.) The necked channels in the center of the α phase are blocked by the two neighboring β phases on each interface whereas the channels near the edge of the α phase reach the crystal surface of $(011)_\alpha$ or $(0-1-1)_\alpha$.

Conclusions

In summary, we observed the bending and straightening transformation of a single crystal in a novel microporous metal complex of $[\text{Cu}(\text{II})_2(1\text{-NA})_4(\text{pyz})_n]$ during the first-order crystal

phase transition induced by step-wise methanol ad- and desorption. In the bent crystal, the α/β interface of $(-12-6)_\alpha // (1-2-6)_\beta$ connected the α and β phases, which have 1D necked channels and nearly isolated voids, respectively, by matching the bending positions and angles of each host 1D chain while minimizing the difference of interchain distances on the interface. Consequently, forming of the most stable connection of each crystal structure with planar interfaces produced anisotropic crystal deformation.

This work was partially supported by a Research Grant, Izumi Science and Technology Foundation for S.T.

Notes and references

^a Department of Nanosystem Science, Graduate School of Nanobioscience, Yokohama City University, 22-2 Seto, Kanazawa-ku, Yokohama, Kanagawa 236-0027, Japan. Fax: +81-045-787-2187; Tel: +81-045-787-2187; E-mail: staka@yokohama-cu.ac.jp

Electronic Supplementary Information (ESI) available: Experimental details and crystallographic data. See DOI: 10.1039/c000000x/

- (a) Y. H. Hu, L. Zhang, *Adv. Mater.*, 2010, **22**, E117–E130; (b) S. Chaemchuen, N. A. Kabir, K. Zhou, F. Verpoort, *Chem. Soc. Rev.*, 2013, **42**, 9304–9332; (c) M. Shah, M. C. McCarthy, S. Sachdeva, A. K. Lee, H.-K. Jeong, *Ind. Eng. Chem. Res.*, 2012, **51**, 2179–2199; (d) J. Y. Lee, O. K. Farha, J. Roberts, K. A. Scheidt, S. T. Nguyen, J. T. Hupp, *Chem. Soc. Rev.*, 2009, **38**, 1450–1459.
- (a) *Introduction to Zeolite Molecular Science and Practice*, 3rd ed., J. Čejka, H. van Bekkum, A. Corma, F. Schüth, Eds. Studies in Surface Science and Catalysis, Vol. 168, Elsevier: Oxford, U.K., 2007; (b) *From Zeolites to Porous MOF Materials*, R. Xu, Z. Gao, J. Chen, W. Yan, Eds. Studies in Surface Science and Catalysis, Vol. 170A, Elsevier: Oxford, U.K., 2007.
- (a) Y. Takashima, V. M. Martínez, S. Furukawa, M. Kondo, S. Shimomura, H. Uehara, M. Nakahama, K. Sugimoto, S. Kitagawa, *Nat. Commun.*, 2011, **2**, 168; (b) A. Alec Talin, A. Centrone, A. C. Ford, M. E. Foster, V. Stavila, P. Haney, R. Adam Kinney, V. Szalai, F. El Gabaly, H. P. Yoon, F. Léonard, M. D. Allendorf, *Science*, 2014, **343**, 66–69; (c) G. J. Halder, C. J. Kepert, B. Moubaraki, K. S. Murray, J. D. Cashion, *Science*, 2002, **298**, 1762–1765; (d) Y. Yue, E. Gao, C. Fang, T. Zheng, J. Liang, C. Yan, *Crystal Growth & Design*, 2008, **8**, 3295–3301.
- (a) R. Kitaura, K. Seki, G. Akiyama, S. Kitagawa, *Angew. Chem. Int. Ed.*, 2003, **42**, 428–431; (b) F. Salles, G. Maurin, C. Serre, P. L. Llewellyn, C. Knöfel, H. J. Choi, Y. Filinchuk, L. Oliviero, A. Vimont, J. R. Long, G. Férey, *J. Am. Chem. Soc.*, 2010, **132**, 13782–13788.
- S. Takamizawa, T. Saito, T. Akatsuka, E. Nakata, *Inorg. Chem.*, 2005, **44**, 1421–1424.
- (a) M. H. Zeng, Y. X. Tan, Y. P. He, Z. Yin, Q. Chen, M. Kurmoo, *Inorg. Chem.*, 2013, **52**, 2353–2360; (b) H. L. Zhou, R. B. Lin, C. T. He, Y. B. Zhang, N. Feng, Q. Wang, F. Deng, J. P. Zhang, X. M. Chen, *Nat. Commun.*, 2013, **4**, 2534.
- (a) S. Takamizawa, E. Nakata, T. Akatsuka, R. Miyake, Y. Kakizaki, H. Takeuchi, G. Maruta, S. Takeda, *J. Am. Chem. Soc.*, 2010, **132**, 3783–3792; (b) S. Takamizawa, C. Kachi-Terajima, M. Kohbara, T. Akatsuka, T. Jin, *Chem. – Asian J.*, 2007, **2**, 837–848; (c)

- S. Takamizawa, Y. Takasaki, R. Miyake, *J. Am. Chem. Soc.*, 2010, **132**, 2862–2863; (d) Y. Takasaki, S. Takamizawa, *J. Am. Chem. Soc.*, 2014, **136**, 6806–6809.
- 8 Introducing pyrazine vapor (0.26 g, 3.3 mmol) into the methanol solution (60 mL) of copper(II) acetate monohydrate (0.102 g, 0.509 mmol) and 1-naphthoic acid (0.859 g, 4.99 mmol) gave blue green single crystals of **1** with a size of 100–500 μm in 30.9% yield (70.1 mg).
- 9 S. Takamizawa, R. Miyake, *CrystEngComm*, 2010, **12**, 2728–2733.
- 10 Crystal data for **1**•0.93(MeOH) at 90 K: Triclinic, *P*-1, $a = 10.7482(17)$ Å, $b = 12.230(2)$ Å, $c = 16.366(3)$ Å, $\alpha = 95.110(3)^\circ$, $\beta = 96.968(3)^\circ$, $\gamma = 102.936(3)^\circ$, $V = 2066.2(3)$ Å³, $Z = 2$, $D_{\text{calc}} = 1.482$ Mg m⁻³, $R_1 = 0.0580$ (0.0701), $wR_2 = 0.1598$ (0.1699) for 8394 reflections with $I > 2\sigma(I)$ (for 10274 reflections (15630 total measured)), goodness-of-fit on $F^2 = 1.062$, largest diff. peak (hole) = 1.468 (–1.016) e Å⁻³; crystal data for **1** at 90 K: Triclinic, *P*-1, $a = 10.4745(11)$ Å, $b = 11.6064(12)$ Å, $c = 17.0370(17)$ Å, $\alpha = 97.583(2)^\circ$, $\beta = 104.918(2)^\circ$, $\gamma = 90.081(2)^\circ$, $V = 1982.5(4)$ Å³, $Z = 2$, $D_{\text{calc}} = 1.494$ Mg m⁻³, $R_1 = 0.0429$ (0.0623), $wR_2 = 0.1139$ (0.1264) for 7440 reflections with $I > 2\sigma(I)$ (for 9616 reflections (14013 total measured)), goodness-of-fit on $F^2 = 1.036$, largest diff. peak (hole) = 0.952 (–0.757) e Å⁻³; crystal data for **1** at 293 K: Triclinic, *P*-1, $a = 10.6065(8)$ Å, $b = 11.6485(9)$ Å, $c = 17.4513(14)$ Å, $\alpha = 80.612(2)^\circ$, $\beta = 75.2125(10)^\circ$, $\gamma = 89.821(2)^\circ$, $V = 2055.1(3)$ Å³, $Z = 2$, $D_{\text{calc}} = 1.441$ Mg m⁻³, $R_1 = 0.0509$ (0.0882), $wR_2 = 0.1365$ (0.1625) for 6592 reflections with $I > 2\sigma(I)$ (for 10052 reflections (15194 total measured)), goodness-of-fit on $F^2 = 1.018$, largest diff. peak (hole) = 0.677 (–0.596) e Å⁻³; CCDC-1038817 to 1038819 contain the supplementary crystallographic data for this paper.
- 11 The occupancy values of two methanol molecules in different voids determined by X-ray data were 0.6 and 0.4.
- 12 The lines along the boundaries remained even after 2 days in saturated pressure of methanol vapor.
- 13 The boundary strain was estimated from the ratio of the averaged cross-sectional area of two square pillars consisting of four neighboring 1D chains on the interface by using averaged interchain distances. ($S_a/S_p = 101.8 \text{ \AA}^2 / 105.6 \text{ \AA}^2 = 0.964$)